Contrib Mineral Petrol (1997) 128: 81–96

Christopher D. Wareham · Ian L. Millar
Alan P.M. Vaughan

The generation of sodic granite magmas, western Palmer Land, Antarctic Peninsula

Received: 2 October 1995 / Accepted: 5 January 1997

Abstract Subduction-related Mesozoic to Cainozoic granites *s.l.* in western Palmer Land, Antarctic Peninsula, have similar chemical compositions to Archean tonalite-trondhjemite-granodiorite (TTG) suites, Phanerozoic slab-melts (adakites), and to experimental partial melts of basaltic material in equilibrium with amphibole ± pyroxene ± garnet. They are predominantly sodic, metaluminous and most have Al_2O_3 > 15 wt% and Y < 18 ppm. All are light rare earth element (LREE)-enriched (2 < La/Yb_n < 30) and most have small Eu anomalies. They have a wide range of initial $\varepsilon Nd_{(t)}$ (−6.8 to +4.5) and $\varepsilon Sr_{(t)}$ (+293.4 to −3.7), but most Pb isotope compositions deviate by < 0.3% from their mean. The Pb isotope data indicate a crustal component to all the granites, which Sr and Nd isotope variations suggest is pre-Triassic–Triassic. The $^{207}Pb/^{204}Pb_{(t)}$ range from 15.602 to 15.666 and appear to preclude a significant Proterozoic, or older, crustal component. The granites have chemical and isotopic compositions that suggest they are not partial melts of subducted oceanic lithosphere, as has been suggested for some Archean and Phanerozoic TTG magmas. We conclude that they were produced by mixing between basaltic-andesitic arc magmas, partial melts of juvenile basaltic lower crust and pre-Triassic crust. The low H(heavy)REE + Y content of some of the granites requires that garnet was a residual phase in the crust during partial melting, indicating a crustal thickness of > 36 km. Between Triassic and Tertiary times the initial $\varepsilon Nd_{(t)}$ of the magmatism increased and $\varepsilon Sr_{(t)}$ decreased, suggesting that new continental crust was produced during this period. Underplating by mafic magma was an important crustal growth mechanism in the arc: the generation of abnormally thick crust, and its subsequent fusion, is considered to be a consequence of ca. ≥ 180 Ma of subduction and associated magmatism in the region. An implication of the model is that dense garnet-amphibolite and eclogite residues from partial melting of the lower crust will accumulate. In theory, the setting was appropriate for such residues to detach from the base of the crust and to sink into the convecting mantle. Such a process would leave the rest of the crust enriched in large ion lithophile elements/LREE, but depleted in HREE + Y.

C.D. Wareham (✉) · A.P.M. Vaughan
British Antarctic Survey, High Cross, Madingley Road, Cambridge CB3 0ET, UK

I.L. Millar
British Antarctic Survey, c/o NERC Isotope Geosciences Laboratory, Keyworth, Nottingham, NG12 5GG, UK

Editorial responsibility: I. Parsons

Introduction

The origin of sodic Phanerozoic arc magmas characterised by unusually low Y (< 18 ppm) and heavy rare earth element [HREE (Yb_n < 8.5)] contents, negligible or positive Eu anomalies, and high Al_2O_3 (> 15 wt%) contents has been the subject of much discussion (Drummond and Defant 1990; Atherton and Petford 1993; Sen and Dunn 1994; Feeley and Hacker 1995; Barnes et al. 1996). Many Pacific margin plutons have these chemical characteristics, including those in the Antarctic Peninsula (Hole 1986; Harrison and Piercy 1990; Wever et al. 1995), Chile (Pichowiak et al. 1990; Weaver et al. 1990), and North America (Miller and Barton 1990; Hawkesworth and Clarke 1994; Barnes et al. 1996). They are also characteristic of Archean tonalite-trondhjemite-granodiorite (TTG) suites, many of which are considered to be melts of subducted oceanic lithosphere, leaving a garnet-bearing residuum (Arth 1979; Martin 1986, 1987). However, widespread melting of subducted oceanic lithosphere is only considered to have been possible in Archean subduction zones because asthenosphere temperatures were hotter then than in the Phanerozoic (Richter 1988). Subducting lithosphere generally dehydrates in Phanerozoic subduction zones before it melts, thereby rehydrating the overlying mantle wedge which subsequently melts to produce calc-alkaline magmas: in the absence of a hydrous component, subducting oceanic lithosphere cannot melt in arc settings (Martin 1986). Oceanic lithosphere can only melt in Phanerozoic subduction zones if it, or the surrounding mantle, is anomalously warm (Peacock et al. 1994). Archean TTG-like volcanic rocks are prominent in Phanerozoic arcs where oceanic lithosphere being subducted at the trench is <25 Ma old (Drummond and Defant 1990; Defant and Drummond 1990). By analogy with Archean TTG magmas, such volcanic rocks are believed to be partial melts of young, therefore relatively warm, subducted oceanic lithosphere, leaving a garnet-bearing residuum (Defant and Drummond 1990). Defant and Drummond (1990) called these rocks adakites, after Adak Island where Kay (1978) first described them.

Despite the association between the subduction of young oceanic lithosphere and the occurrence of Archean TTG-like volcanic rocks, experimental studies suggest that only some of their characteristics can be acquired by magmas produced during melting of a NMORB ("normal" mid-ocean ridge basalt) protolith (Rapp et al. 1991; Rushmer 1991; Sen and Dunn 1994; Rapp and Watson 1995). Moreover, thermal modelling suggests that these magmas can only be generated from subducted oceanic lithosphere that is younger than ca. 5 Ma old at the trench (Peacock et al. 1994; Molner and England 1995), not ca. 25 Ma old as suggested by Drummond and Defant (1990). Uncertainty regarding the origin of Archean TTG-like magmas is further compounded by the presence of adakites in the Andean volcanic chain, where the subducted slab was substantially older than 25 Ma at the time of magmatism. For example, Miocene–Pliocene volcanic rocks of the Cordillera Blanca (Peru) were produced above ca. 60 Ma old subducted oceanic lithosphere and are considered to be partial melts of recently accreted (i.e. warm) garnet-bearing basaltic lower crust (Atherton and Petford 1993). Elsewhere in the Andes, adakitic volcanic rocks were produced when mantle wedge magmas assimilated garnet-bearing lower crustal gneisses (Hildreth and Moorbath 1988; Feeley and Davidson 1994; Feeley and Hacker 1995).

In this paper, we discuss the genesis of subduction-related granites *s.l.* along the south-western margin of the Antarctic Peninsula, in western Palmer Land (Fig. 1). One hundred and fifty-six samples were collected from 34 intrusive centres in an area of ca. 15000 km^2. Much of the magmatism is Cretaceous in age, although Triassic, Jurassic and Tertiary intrusions are present (Leat et al. 1995; I.L. Millar unpublished data). Over half of the intrusions sampled have chemical characteristics typical of adakite and Archean TTG suites, with Al_2O_3 > 15 wt%, Y < 18 ppm, and Sr/Y > 40 (Drummond and Defant 1990). These data are discussed within the context of models for the generation of Archean TTG and adakite melts.

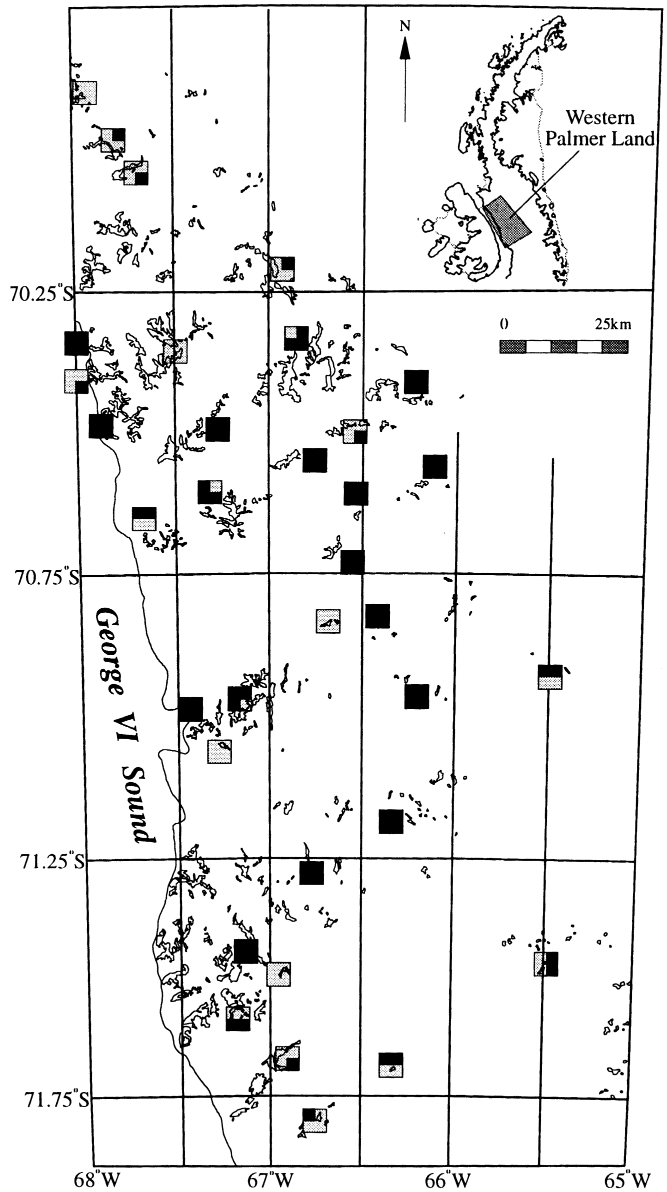

Fig. 1 Distribution of "adakites" and "non-adakites" (as defined by Y and Sr/Y) in western Palmer Land. *Symbols* indicate the approximate volumetric proportions of both magma types. (*Black fill* adakite; *grey fill* non-adakite). *Inset* shows location of the study area

Geological background

The Antarctic Peninsula (Fig. 2) was a site of subduction-related magmatism for much of the Mesozoic and Cainozoic (Suárez 1976; Saunders et al. 1980). Subduction along the proto-Pacific margin of Gondwana occurred from at least the Middle Triassic (Pankhurst 1990; Storey et al. 1992) and locally there is evidence for Paleozoic subduction (Pankhurst 1982; Milne and Millar 1989). Subduction ceased along much of the Antarctic Peninsula between ca. 50 Ma and the present, following a series of northwards younging ridge-trench collisions (Barker 1982; Larter and Barker 1991). There is no unequivocal evidence to suggest that Mesozoic subduction was continuous. The occurrence of Middle Jurassic high-MgO andesites in the northern Antarctic Peninsula led Alabaster and Storey (1990) to conclude that a mid-ocean ridge system was present near the

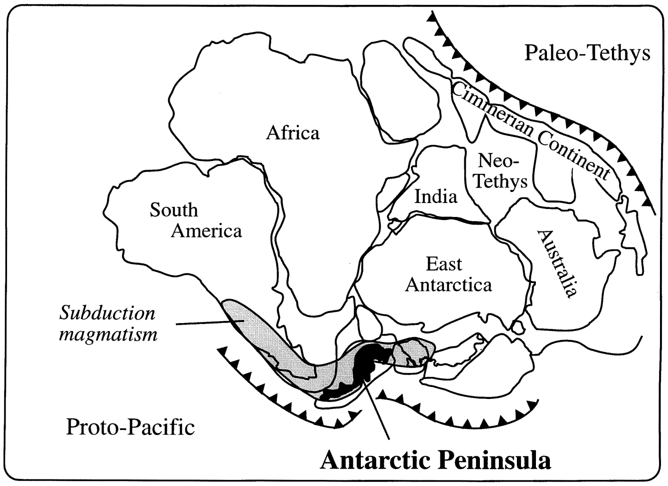

Fig. 2 Pre-break-up Late Triassic–Early Jurassic Gondwana reconstruction illustrating the relative positions of the various crustal blocks and positions of the subduction-related magmatic belt (after Storey et al. 1992)

peninsula during the Jurassic and that young, warm, ocean floor was being subducted. It is conceivable that these andesites were formed prior to, or during, ridge-trench collision. Late Cretaceous high-MgO andesites in the fore-arc may have a similar origin (McCarron 1995).

Granite *s.l.* magmas were emplaced in western Palmer Land (Fig. 1) from Late Triassic times through to the earliest Tertiary, when subduction stopped in the area (Barker 1982; Harrison and Piercy 1990; I.L. Millar unpublished data). Plutons that have not been dated directly have their emplacement ages constrained by field relationships with dated intrusions and tectonic events. The most reliable intrusion ages are U-Pb zircon ages (Vaughan and Millar 1996; I.L. Millar unpublished data), although Rb-Sr whole rock (Harrison 1989; I.L. Millar unpublished data) and mineral K-Ar (Rex 1976; C.D. Wareham unpublished data) ages have been determined. As in eastern Palmer Land (Wever et al. 1994), the western Palmer Land granites *s.l.* (WPLG) locally intruded pre-Late Triassic paragneisses of unknown protolith age. The oldest known basement in the Antarctic Peninsula is Silurian (Milne and Millar 1989), although intrusions with Proterozoic Nd model ages (Table 1) and zircons with inherited cores (Loske and Miller 1991; I.L. Millar unpublished data) suggest that some may be older.

The WPLG are predominantly fine to medium grained quartz-diorites, tonalites and granodiorites, although quartz-monzodiorites and monzogranites (Le Maitre 1989) are present. Albite generally occurs in the groundmass and is present as anhedral–subhedral crystals up to 5 mm across. Multiple twinning is common. Arcuate twins, undulose extinction and dislocations across twin-planes suggest that some twinning is strain-induced. Oligocene–andesine (An_{26-49}) commonly forms 1 to 5 mm, anhedral–subhedral, phenocrysts with zoning and twinning textures that suggest complex crystallisation histories. These phenocrysts have normal and reverse zoning and some are mantled composites of crystal fragments. Some have corroded rims. Lamellar and pericline twinning is common and in places is discontinuous with the zoning. The proportion of albite to oligocene–andesine is variable throughout the suite. Micro-perthitic potassium feldspar is a minor component and generally comprises <10 modal%, where it occurs as a sub-mm interstitial phase. In the few samples where potassium feldspar content exceeds 20%, it also occurs as subhedral phenocrysts up to 5 mm across.

Hornblende and biotite are the dominant mafic silicates. Hornblende forms 1 to 4 mm subhedral phenocrysts and rarely comprises more than ca. 25% of any sample. Some hornblende is poikilitic and contains partially resorbed clinopyroxene cores, suggesting that it only became a liquidus phase late in the crystallisation sequence. Biotite appears to have replaced hornblende where they occur together. In sections where biotite is the only mafic silicate, it comprises $<15\%$ of the rock and forms 1 to 3 mm anhedral crystals. Accessory minerals include apatite, titanite, magnetite and zircon. Titanite is particularly conspicuous and subhedral–anhedral crystals are up to 5 mm long in some intrusions.

Many WPLG contain mafic inclusions up to ca. 1 m in size. These are sub-spherical to extremely elongate and asymmetric and in some cases are contiguous with disrupted, syn-plutonic, mafic dykes. Textures suggestive of magma mingling and magma mixing between inclusions and their hosts are abundant, particularly where gabbro and granite occur in close association. Inclusions with chilled and irregular margins have an origin that is consistent with magma mingling (cf. Moyes 1986; Vaughan et al. 1995; Vaughan and Millar 1996). Ghost-like inclusions and those with diffuse margins or schlieren textures appear to have been incompletely mixed with their host magma.

Major crustal shear zones controlled the emplacement of many WPLG, which are consequently variably deformed (e.g. Vaughan and Millar 1996). Deformation textures range from strongly aligned, "tiled" (Paterson et al. 1989) feldspar and hornblende phenocrysts, to protomylonite with ductile deformation of hornblende grains. Some plutons were deformed syn-magmatically in coeval mylonite zones and grain-scale structures and deformed mafic inclusions suggest dextral or normal simple shear during pluton emplacement (Vaughan and Millar 1996). Subtle deformation features include strain-induced twinning of albite, and strained quartz.

Analytical procedures

Powders for geochemical analysis were prepared from 3–5 kg fresh rock. Samples were reduced to ca. 3 cm^3 chips with a hardened-steel hydraulic splitter, then crushed using a hardened-steel fly press. A ca. 200 g aliquot of <1200 μm sample was subsequently powdered using an agate swing mill. The REE plus Sc, Ta, Hf, Th and U concentrations were determined by INAA at the Open University (Potts 1987). Most of the remaining trace and major element concentrations were determined by XRF at Keele University (Floyd 1985). Isotope analyses were carried out at the NERC Isotope Geosciences Laboratory. The Sr, Sm and Nd isotope compositions, and corresponding Sr, Rb, Sm and Nd concentrations, were determined using standard techniques (e.g. Pankhurst and Rapela 1995). Ratios of $^{87}Sr/^{86}Sr$ are normalised to $^{86}Sr/^{88}Sr = 0.1194$. Repeated analyses of NBS987 during the course of this study gave $^{87}Sr/^{86}Sr = 0.710190$. Ratios of $^{143}Nd/^{144}Nd$ are normalised to $^{146}Nd/^{144}Nd = 0.7219$. Repeated analyses of Johnson-Matthey Nd yielded $^{143}Nd/^{144}Nd = 0.511122$, corresponding to 0.511858 for the La Jolla standard. Multi-stage (T_{DM}') depleted mantle Nd model ages were calculated using the equation of DePaolo et al. (1991). The Pb isotope ratios were determined on hand-picked plagioclase and potassium feldspar separates that were leached in concentrated HCl and then 5% HF-HBr in order to remove as much non-structurally bound Pb as possible (cf. Gariépy and Allègre 1985). The feldspars were dissolved in HF-HNO_3 and the Pb separated and purified using Dowex 1×8 200–400 mesh resin (Hole et al. 1993). The Pb isotope compositions were analysed on a Finnigan MAT 262 multi-collector mass spectrometer in static mode. Repeated analyses of NBS981 yielded $^{206}Pb/^{204}Pb$, $^{207}Pb/^{204}Pb$, and $^{208}Pb/^{204}Pb$ of 16.906, 15.463, 36.559 respectively. Quoted Pb isotope ratios are corrected for mass fractionation using the preferred values of Catanzaro et al. (1968). Maximum procedural blanks throughout the course of this study were <300 pg for Pb, Nd, and Sr.

Compositional characteristics

The following discussion focuses upon a representative subset of 39 granite samples, including appropriate ones

Table 1 Western Palmer Land granites and mafic dykes

Sample #	Granites													
	R.5278.9	R.5257.1	R.5297.3	R.5280.2	R.2432.1	R.2556.1	R.5270.1	R.5271.4	R.5278.12	R.3238.1	R.5287.1	R.6063.5	R.6308.1	R.6314.9
SiO_2	68.43	75.2	72.49	68.76	64.24	62.17	57.76	64.41	75.07	64.58	66.7	54.5	69.83	61.43
TiO_2	0.39	0.12	0.48	0.74	0.62	0.51	0.82	0.68	0.08	0.52	0.55	0.69	0.57	0.72
Al_2O_3	15.32	13.6	14.06	14.38	16.28	18.23	16.41	17.12	13.64	17.61	15.78	17.34	13.75	17.06
Fe_2O_3	3.24	0.49	2.36	4.14	5.02	6.01	7.32	3.96	0.72	3.65	4.23	9.08	4.58	5.54
MnO	0.04	0	0.03	0.06	0.06	0.11	0.15	0.04	0.01	0.05	0.07	0.15	0.07	0.1
MgO	1.39	0.1	0.62	1.11	1.61	2.52	4.62	1.08	0.01	1.17	1.43	4.6	0.69	2.91
CaO	2.07	0.92	1.9	2.88	4.62	6.45	7.24	3.11	1.01	5.08	4.39	9.12	1.36	5.75
Na_2O	4.35	2.31	3.52	3.04	3.8	3.33	3.37	4.83	3.31	5.11	3.87	3.37	2.57	4.05
K_2O	3.85	6.57	3.64	4.4	1.42	1.74	1.27	3.73	5.42	1.51	2.01	0.72	5.77	1.41
P_2O_5	0.15	0	0.02	0.16	0.2	0.19	0.14	0.18	0	0.18	0.12	0.1	0.1	0.19
Total	99.23	99.31	99.12	99.67	97.87	101.26	99.1	99.14	99.27	99.46	99.15	99.67	99.29	99.16
Rb	166	179	12	136	41	56	46	91	194	42	77	19	174	38
Sr	520	193	318	319	585	643	380	455	237	884	384	290	240	571
Y	25	7	18	43	9	17	21	41	5	13	16	22	37	13
Nb	10	1	9	15	3	9	5	14	1	5	5	3	12	5
Zr	148	57	203	260	233	126	103	374	66	127	146	38	326	129
Ni	13	1	5	4			27	3	0	0	2	19	3	18
Cr	33	7	12	6		28	64	7	0	0	0	46	11	39
V	55	8	39	67	100		182	32	3	56	74	250	32	102
Ba	1037	958	833	1065	889	631	398	1638	454	600	466	132	1561	510
Th				13.7	2.43	4.3	5.43	12.4	20	3.91	9.28	2.08	25.94	3.74
U				1.8	0.8	1.4	2.1	3.3	0.9	1.4	3.2	0.6		
Ta					0.24					0.4	0.81	0.09	0.74	0.4
Hf				8.37	6.05	3.62	3.02	10.4	2.42	3.37	3.86	1.62	10.18	3.5
Sc				10.6	3.3	12.3	22.8	7.2	1	4.8	8.6	28.5	11.8	11.4
La				42	16.9	18.8	16.4	69.2	18.5	18.8	22.6	8.1	71.5	19.6
Ce				89	30.5	37.6	32.9	144	34.4	37.9	40.1	18.3	149	41.2
Nd				41.4	12.6	18.9	17.8	62.2	13.1	18.6	17.2	10.7	66.8	19.1
Sm				8.66	2.09	3.96	4.01	11.9	2.92	3.27	3.63	2.95	12.5	3.52
Eu				1.43	1.15	1.06	1.08	2.23	0.63	0.89	0.97	0.92	1.92	0.99
Tb				1.23	0.23	0.53	0.62	1.39	0.23	0.35	0.45	0.58	1.46	0.43
Yb				4.04	0.76	1.58	2.06	4	0.41	0.95	1.56	2.13	3.21	1.28
Lu				0.6	0.12	0.23	0.31	0.56	0.07	0.13	0.24	0.33	0.47	0.19
$^{87}Sr/^{86}Sr_i$	0.70669	0.72257	0.71220	0.70806	0.70679	0.70647	0.70586	0.70642	0.70876	0.70585	0.70562	0.70448	0.70973	0.70574
εSr_i	+34.9	+293.4	+112.9	+54	+35.9	+31.4	+22.4	+30.3	+63	+21.6	+18.3	+2.1	+76.6	+19.9
$^{143}Nd/^{144}Nd_i$	0.51216	0.51234	0.51218	0.51219	0.51232	0.51227	0.51238	0.51234	0.51230	0.51241	0.51241	0.51259	0.51211	0.51239
εNd_i	−3.7	−0.1	−3.6	−3.7	−1.1	−2.0	−0.4	−1.3	−1.3	−0.9	−0.8	+2.6	−6.8	−1.5
T_{DM}* (Ma)	1120	857	1095	1106	916	979	845	910	995	853	848	594	1283	893
$^{206}Pb/^{204}Pb$	18.701				18.735		18.638	18.636		18.678	18.675			
$^{207}Pb/^{204}Pb$	15.672				15.648		15.644	15.645		15.631	15.635			
$^{208}Pb/^{204}Pb$	38.630				38.541		38.461	38.475		38.641	38.506			
Age (Ma)	227[a]	227[a]	211[a]	203[a]	203[a]	203[c]	182[a]	183[a]	150[b]	141[a]	141[a]	141[a]	140[c]	135[c]

Table 1 (Continued)

Sample #	Granites										Mafic dykes			
	R.6315.8	R.6316.4	R.5796.4	R.2414.3	R.5966.2	R.2418.4	R.2480.1	R.5736.1	R.5902.8	R.5256.1	R.5748.1	R.5748.14	R.5784.2	R.5717.3
SiO_2	78.5	54.65	57.14	71.24	66.15	69.11	56.99	65.57	59.51	64.34	48.70	53.52	51.84	47.68
TiO_2	0.09	0.94	0.79	0.39	0.46	0.36	0.99	0.47	0.78	0.53	0.95	0.93	0.93	0.79
Al_2O_3	11.65	18.42	17.93	14.14	16.14	15.86	15.98	15.71	17.59	15.91	19.72	19.23	18.74	15.20
Fe_2O_3	1.1	8.37	6.54	3.63	4.23	3.72	9.71	4.17	6.58	5.04	10.75	7.69	8.47	10.31
MnO	0.01	0.13	0.1	0.09	0.06	0.1	0.2	0.07	0.1	0.08	0.27	0.12	0.12	0.17
MgO	0	4.46	4.2	0.85	1.88	0.95	3.67	1.79	2.94	2.18	4.29	3.71	4.70	10.96
CaO	0.43	8.38	7.22	2.85	3.75	3.69	5.52	3.85	6.19	4.53	6.46	8.34	9.85	11.91
Na_2O	3.75	3.27	3.97	4.03	3.78	4.63	3.59	3.82	3.95	3.39	2.07	4.32	4.05	1.73
K_2O	4.48	0.92	1.6	2.46	2.74	1.26	2.17	3.3	1.94	3.34	3.42	1.56	0.16	0.59
P_2O_5	0	0.23	0.26	0.1	0.15	0.11	0.35	0.14	0.25	0.13	0.26	0.23	0.39	0.07
Total	100.01	99.77	99.75	99.78	99.34	99.79	99.17	98.89	99.83	99.47	96.89	99.65	99.25	99.41
Rb	191	25	39	84	135	41	72	80	61	107	153	63	2	13
Sr	27	691	1059	163	584	296	550	578	649	449	371	730	1196	320
Y	53	14	10	35	12	18	29	13	16	22	22	18	29	16
Nb	19	4	4	5	8	4	10	8	5	7	7	6	7	5
Zr	123	70	61	145	122	129	205	123	117	156	120	112	111	56
Ni	2	20	30	0	6		5	6	12	9	19	20	17	160
Cr	10	38	76	0	16		23	69	16	3	36	37	25	538
V	1	193	155	37	72	46	165	86	134	112	214	198	254	234
Ba	176	314	747	469	898	450	916	1001	701	840	721	486	296	31
Th	19.4	1.93	2.3	9.59	14.8	4.07	3.74	16.8	5.61	17	1.5	1.9	7.9	0.4
U		0.5	0.5	1.9	4	1.5		2.6	0.8	3.9	1.0	0.5	2.0	0.4
Ta	1.57	0.21	0.36	0.95	0.97	0.63		0.99	0.52		0.2	0.3	0.3	0.1
Hf	5.6	2.13	2.96	4.8	4.48	3.94	5.99	3.9	3.53	4.98	3.1	3.3	3.2	1.4
Sc	3.1	18.1	14.4	8.1	7.7	8.7	19.4	9.5	13.2	14	22.7	21.1	26.0	40.6
La	24.8	12.7	24.5	19.2	26.7	16.2	23.9	33	22.1	33.6	16.0	19.6	39.5	3.7
Ce	57.7	27.8	48.8	38.2	47.1	28.4	58.3	61.7	45.9	68	35.2	40.4	82.2	9.6
Nd	35.4	15.4	22.9	18.3	19.6	13.7	31.6	25.5	22.3	31.1	22.1	21.6	47.8	6.9
Sm	9.99	3.3	3.93	4.1	3.93	2.88	6.47	4.51	4.25	6.15	4.9	4.6	10.3	1.9
Eu	0.44	1.03	1.2	0.96	0.92	0.99	1.49	1.09	1.13	1.08	1.3	1.3	2.6	0.8
Tb	1.62	0.46	0.4	0.72	0.45	0.46	0.84	0.44	0.54	0.64	0.7	0.6	1.1	0.5
Yb	4.82	1.23	0.84	3.89	1.31	1.59	2.62	1.44	1.39	2.29	2.0	1.6	2.1	1.6
Lu	0.66	0.18	0.13	0.64	0.21	0.24	0.38	0.22	0.21	0.34	0.3	0.3	0.3	0.3
$^{87}Sr/^{86}Sr_i$	0.71863	0.70568	0.70678	0.70506	0.70478	0.70492	0.70658	0.70414	0.70636	0.70430	0.70721	0.70633	0.70492	0.70379
εSr_i	+202.9	+19.1	+34.2	+9.6	+5.7	+7.7	+30.8	+3.7	27.9	−1.9	40.0	27.9	7.2	−7.7
$^{143}Nd/^{144}Nd_i$	0.51221	0.51240	0.51233	0.51266	0.51264	0.51254	0.51246	0.51277	0.51238	0.51273	0.51248	0.51240	0.51278	0.51277
εNd_i	−5	−1.2	−3.1	+2.9	+2.5	+.6	−1.5	+4.5	−2.8	+3.3	−0.8	−1.8	4.6	6.1
T_{DM}* (Ma)	1146	873	991	542	572	711	852	410	947	481	805	899	398	340
$^{206}Pb/^{204}Pb$			18.751					18.719	18.793					
$^{207}Pb/^{204}Pb$			15.634					15.608	15.637					
$^{208}Pb/^{204}Pb$			38.520					38.451	38.558					
Age (Ma)	135[c]	135[c]	112[c]	100[c]	100[c]	100[c]	80[b]	80[c]	86[c]	60[b]	91[d]	115[d]	72[d]	140[c]

[a] U-Pb zircon age (I.L. Millar unpublished data)
[b] Rb-Sr whole rock age (I.L. Millar unpublished data)
[c] Ages estimated from cross-cutting/field relationships
[d] K-Ar mineral ages (C.D. Wareham unpublished data)

Table 2 Partition coefficients

	Hornblende	Clinopyroxene	Garnet
La	0.2[b]	0.0515[a]	0.016[d]
Yb	1.7[b]	0.633[a]	3.88[a]
Sc	4.2[c]	0.808[a]	2.62[a]
Sr	0.36[b]	0.157[a]	0.0099[a]
Y	1.9[b]	0.03[b]	16[b]
Rb	0.3[d]	0.001[d]	0.0007[d]
K	1[d]	0.007[a]	0.0002[a]

[a] Hauri et al. 1994
[b] Martin 1987
[c] Henderson 1982
[d] Green 1994

from the study of Harrison and Piercy (1990), for which REE and isotope compositions were determined (Table 1).

The WPLG are calcic to alkalic and medium- to high-K (Fig. 3) with between ca. 55 and 75 wt% SiO_2. Most are metaluminous [0.7 < mol; $Al_2O_3/(Na_2O+K_2O+CaO) < 1.1$] and sodic ($Na_2O/K_2O$ up to 7). The Al_2O_3 contents range from ca. 12 to 19 wt%, with an average of 15.9 wt%. The MgO, Cr, and Ni contents are generally less than 3 wt%, 40 ppm and 20 ppm respectively. Elements Rb, K and Th increase with increasing SiO_2 from ca. 20 to 180 ppm, ca. 1.5 to 6.8 wt% and ca. 2 to 25 ppm respectively. In contrast, Sr concentrations decrease with increasing SiO_2 from ca. 1000 to 200 ppm. The Ba contents vary between ca. 100 and 2000 ppm. The Ta, Nb and Y contents are generally < 1 ppm, < 15 ppm and < 30 ppm respectively. The TiO_2 contents range from 0.08 to 0.99 wt%. The WPLG are typical of convergent margin magmas in that they have high LILE (large ion lithophile element) contents relative to the HFSE (high field strength elements) (Fig. 4). Most have relatively smooth, L(light)REE-enriched, chondrite-normalised REE profiles (Fig. 5) with La/Yb_n

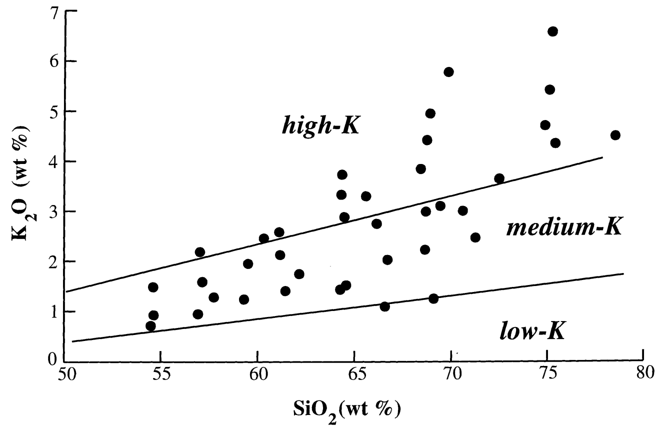

Fig. 3 Plot of K_2O verses SiO_2 (values in wt%). Fields are those of Peccerillo and Taylor (1976)

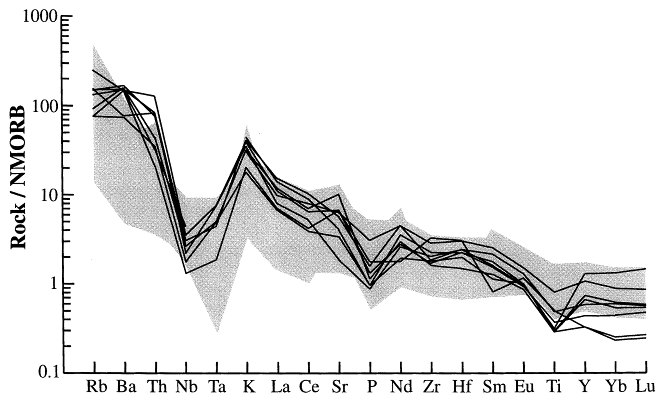

Fig. 4 NMORB normalised (values from Sun and McDonough 1989) trace element abundances of selected western Palmer Land granites. The compositions of contemporaneous basaltic dykes in the region are shown in *stipple* (C.D. Wareham unpublished data)

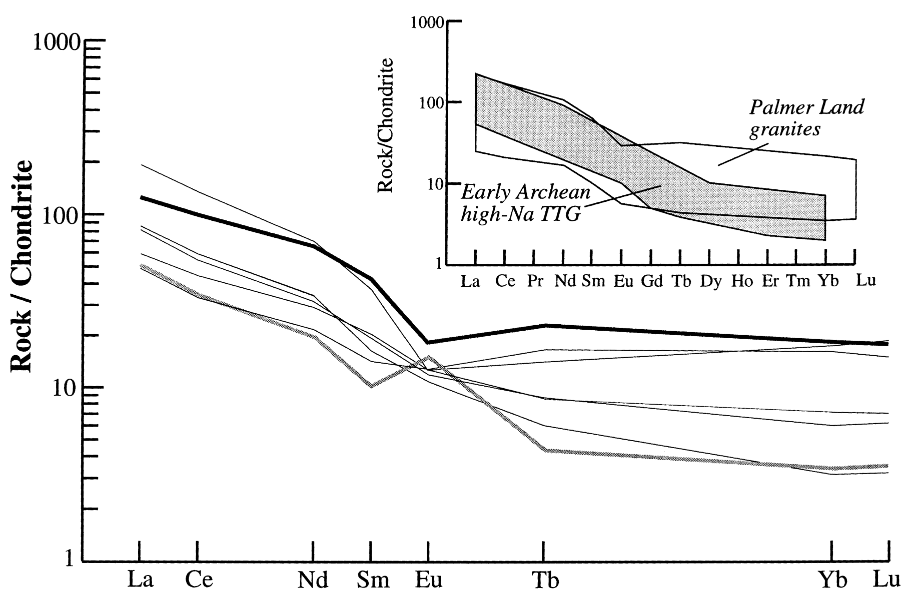

Fig. 5 Chondrite normalised (values from Nakamura 1974) REE abundances of selected western Palmer Land granites. Note the extreme Eu/Eu* of samples R.2432.1 (*stipple*) and R.5280.2 (*heavy black line*). The *inset* contrasts the chondrite-normalised REE compositions of all the western Palmer Land granites with those of early Archean TTG (Taylor and McLennan 1985)

between 2 and 30. Most Eu anomalies (Eu/Eu*) are small, normally 1 ± 0.2, although extreme negative and positive anomalies are present (Fig. 5). There is some compositional overlap between the WPLG and Archean TTG suites, although Archean intrusions have a lower average HREE (Fig. 5 inset) and K_2O content.

Initial $^{87}Sr/^{86}Sr_{(t)}$ and $^{143}Nd/^{144}Nd_{(t)}$ range from ca. 0.704 to 0.723 and ca. 0.5128 to 0.5121 respectively, equivalent to a range in initial $\varepsilon Sr_{(t)}$ of -3.7 to $+293.4$ and $\varepsilon Nd_{(t)}$ of $+4.5$ to -6.8 (Fig. 6). Isotope compositions are independent of Sr and Nd content, but do vary with pluton age. The youngest WPLG generally have the lowest $^{87}Sr/^{86}Sr_{(t)}$ and highest $^{143}Nd/^{144}Nd_{(t)}$ (Fig. 7). Decreasing $^{87}Sr/^{86}Sr_{(t)}$ with decreasing pluton age is a peninsula-wide phenomenon (Pankhurst 1982). The Sr and Nd isotope data are consistent with the WPLG being mixtures of a high-εNd and low-εSr magma source, such as NMORB, and a low-εNd and high-εSr component, such as pre-Triassic continental crust (Fig. 6). Such a mixing origin has been suggested for other, isotopically comparable, Triassic–Tertiary granites *s.l.* in the Antarctic Peninsula (Fig. 6; Pankhurst 1982; Pankhurst et al. 1988; Hole et al. 1991; Wever et al. 1994; Wever et al. 1995).

The WPLG have a restricted range of Pb isotope ratios. The $^{206}Pb/^{204}Pb$ range from 18.635 to 18.793, $^{207}Pb/^{204}Pb$ from 15.607 to 15.672, and $^{208}Pb/^{204}Pb$ from 38.451 to 38.641 (Fig. 8). These ratios deviate by $<0.3\%$ from their mean, and analytical reproducibility is estimated at $\pm 0.1\%$. The data appear to rule out the involvement of Proterozoic crust, which we would expect to have low $^{207}Pb/^{204}Pb$ and $^{206}Pb/^{204}Pb$.

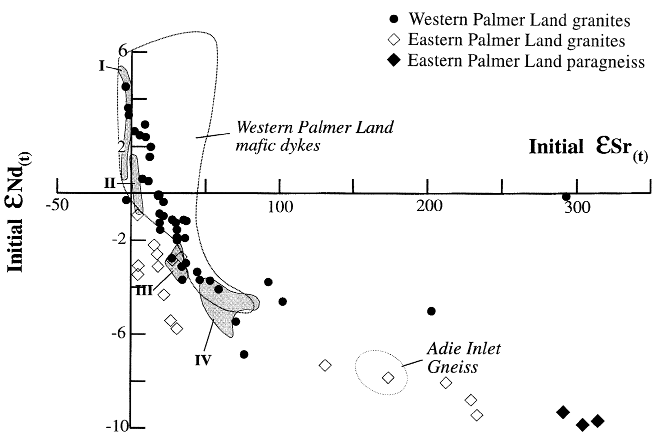

Fig. 6 Initial $\varepsilon Sr_{(t)}$ versus initial $\varepsilon Nd_{(t)}$ for the western Palmer Land granites. Also shown are the compositions of: eastern Palmer Land granites and paragneiss (Wever et al. 1994); granite groups I, II, III and IV from Graham Land, north of Palmer Land, (as defined by Hole et al. 1991); Jurassic Adie Inlet Gneiss, Graham Land (Hole 1986); basaltic dykes in western Palmer Land (C.D. Wareham unpublished data)

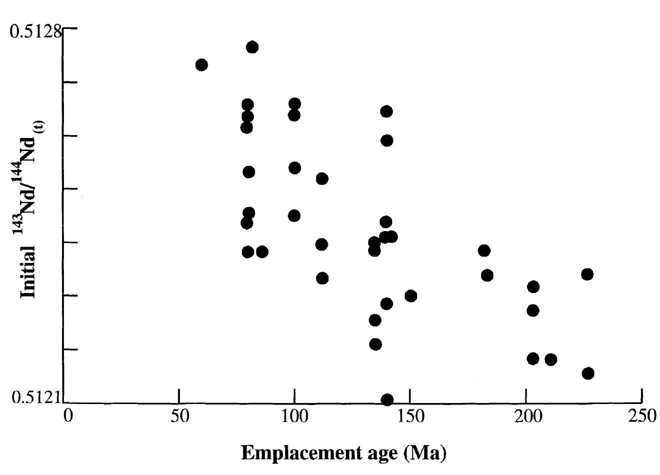

Fig. 7 Pluton emplacement age against initial $^{143}Nd/^{144}Nd_{(t)}$

Magma sources

Models that have been proposed for the generation of Phanerozoic arc magmas with adakite characteristics invoke partial melting of subducted oceanic lithosphere (Drummond and Defant 1990; Defant et al. 1991; Sajona et al. 1993; Kay et al. 1993), fractionation and contamination of mantle wedge magmas within garnet-bearing lower continental crust (Hildreth and

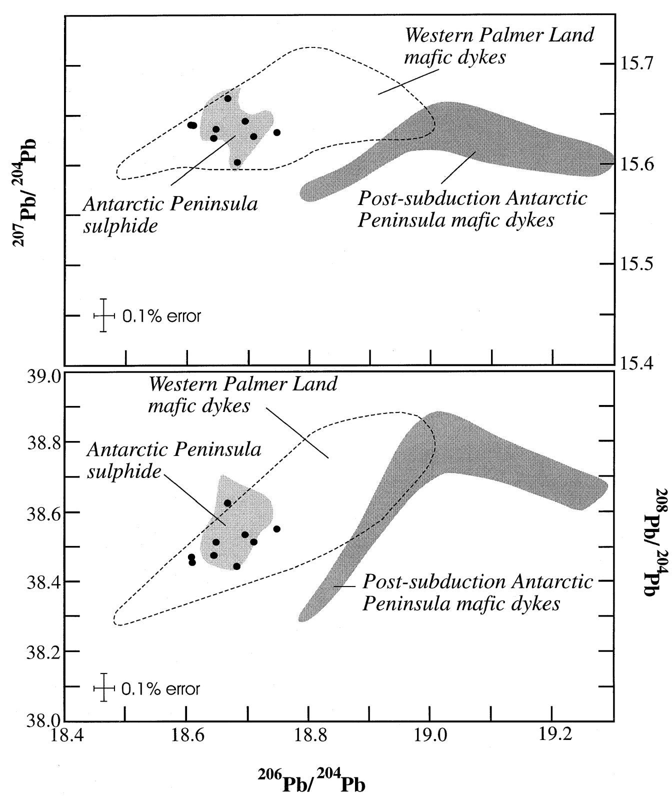

Fig. 8 Pb isotope compositions of the western Palmer Land granites. Also shown are the compositional fields for Antarctic Peninsula sulphide (Willan and Swainbank 1995), post-subduction alkalic basalts (Hole et al. 1993), and basaltic dykes in western Palmer Land (C.D. Wareham unpublished data)

Moorbath 1988; Feeley and Davidson 1994; Feeley and Hacker 1995) and partial melting of magmatically accreted, garnet-bearing, basaltic lower crust (Atherton and Petford 1993; Muir et al. 1995). The applicability of these models to the genesis of the WPLG is evaluated below.

Subducted oceanic lithosphere

Experimental studies demonstrate that basaltic crust and pelagic sediment can be melted at subduction zone pressures and temperatures (Helz 1976; Rushmer 1991; Rapp et al. 1991; Nichols et al. 1994; Peacock et al. 1994; Sen and Dunn 1994; Wolf and Wyllie 1994; Rapp and Watson 1995; Winther 1996). Studies of mantle xenoliths entrained within some Phanerozoic arc basalts suggest that such melts can be an important metasomatising agent within the mantle wedge (Maury et al. 1992; Kepezhinskas et al. 1995; Schiano et al. 1995). Nevertheless, thermal models of Phanerozoic subduction zones suggest that arc magmas can be produced from whole-scale melting of subducted oceanic lithosphere only in exceptional circumstances, such as when the slab is young (Drummond and Defant 1990; Davies and Stevenson 1992; Peacock et al. 1994; Molner and England 1995). Inasmuch as it is not known if Mesozoic subduction along the Antarctic Peninsula was continuous, or if young (<25 Ma; cf. Defant and Drummond 1990) oceanic lithosphere was periodically subducted (cf. Alabaster and Storey 1990), it is necessary to consider subducted oceanic lithosphere as a potential magma source.

Melt and residuum compositions generated during partial melting of a basaltic protolith vary with pressure, temperature and protolith water content (references above). For instance, the Al_2O_3 contents of the experimental melts increase with pressure. At 8 kbar, melt Al_2O_3 is < 15 wt%, and the restite comprises amphibole, plagioclase and orthopyroxene. At > 16 kbar, the melts have > 15 wt% Al_2O_3, and clinopyroxene, amphibole, plagioclase and garnet are residual phases (Rapp et al. 1991). At 20 to 30 kbar, the melts are in equilibrium with a plagioclase-poor or -absent, garnet-bearing amphibolite or eclogite residuum (Rapp et al. 1991; Wolf and Wyllie 1993; Sen and Dunn 1994; Rapp and Watson 1995). The highest pressure partial melts will have the lowest Y, Sc, and HREE contents, but the highest Sr contents and Sr/Y (Rapp and Shimizu 1995). These features are considered to be diagnostic of partial melts of subducted oceanic lithosphere (Martin 1986; Drummond and Defant 1990; Schiano et al. 1995) and characterise some of the WPLG (e.g. Figs. 9 and 10). An amphibole-bearing source for the WPLG is consistent with their low-Ti and -Y contents and low K/Rb, despite their high absolute K and Rb contents. Those with the lowest Y and HREE contents and highest Sr/Y generally have the highest Al_2O_3 content, the most positive Eu/Eu* (Fig. 11) and include the most metaluminous compositions; all these characteristics would be expected for partial melts of a basaltic protolith at pressues > 16 kbar. Nevertheless, although many WPLG have features that are consistent with them being slab melts (e.g. Figs. 9 and 10), they have isotopic (Fig. 6) and some chemical (Figs. 10, 12 and 13) compositions that are significantly different from melts of NMORB-like material. Most experimental melts produced under water-undersaturated and water-saturated conditions and high *P–T* appropriate to subduction zones are trondhjemites and tonalites. These melts are generally richer in Na_2O and poorer in MgO than the WPLG (Figs. 10 and 13). Quartz-monzonite and granodiorite have been synthesised under water-saturated conditions at lower pressures (5 kbar), but are still much poorer in MgO than the WPLG (Helz 1976).

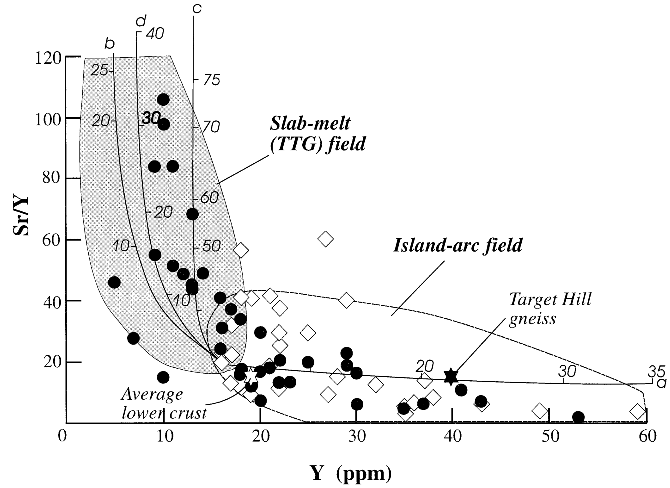

Fig. 9 Plot of Y versus Sr/Y for the western Palmer Land granites (*filled circles*), basaltic dykes (*diamonds*), average lower crust of Taylor and McLennan (1995) and Target Hill gneiss (Milne 1990). AFC trajectories are for clinopyroxene (*a*) 0.7 clinopyroxene 0.3 garnet (*b*) hornblende (*c*), and 0.7 hornblende 0.3 garnet (*d*). AFC modelled using an assimilation:crystallisation ratio of 0.7 and an initial magma composition of R.5717.3 (Table 1). Contaminant has 40 ppm Y and 360 ppm Sr. Partition coefficients as per Table 2. "Slab-melt (TTG)" and "island arc" fields are taken from Drummond and Defant (1990)

Compositional differences between the WPLG and experimental partial melts of basalt could reflect the interaction of slab-derived magmas with mantle wedge peridotite. For example, Kay et al. (1993) and Hochstaedter et al. (1994) argued that this could account for the "anomalously" high MgO, Ni and Cr contents of proposed slab-derived magmas. However, theoretical (Davies and Stevenson 1992) and xenolith (Kepezhinskas et al. 1995; Schiano et al. 1995) studies suggest that low temperature (ca. 900 °C) slab-melts are likely to "freeze" and vein the sub-arc mantle. Mafic arc magmas derived from such mantle may inherit a slab-melt signature (Schiano et al. 1995) and it is possible that some adakitic magmas are simply fractionates of these (Stern and Hanson 1990). However, we do not consider this scenario to apply to the WPLG. There are no

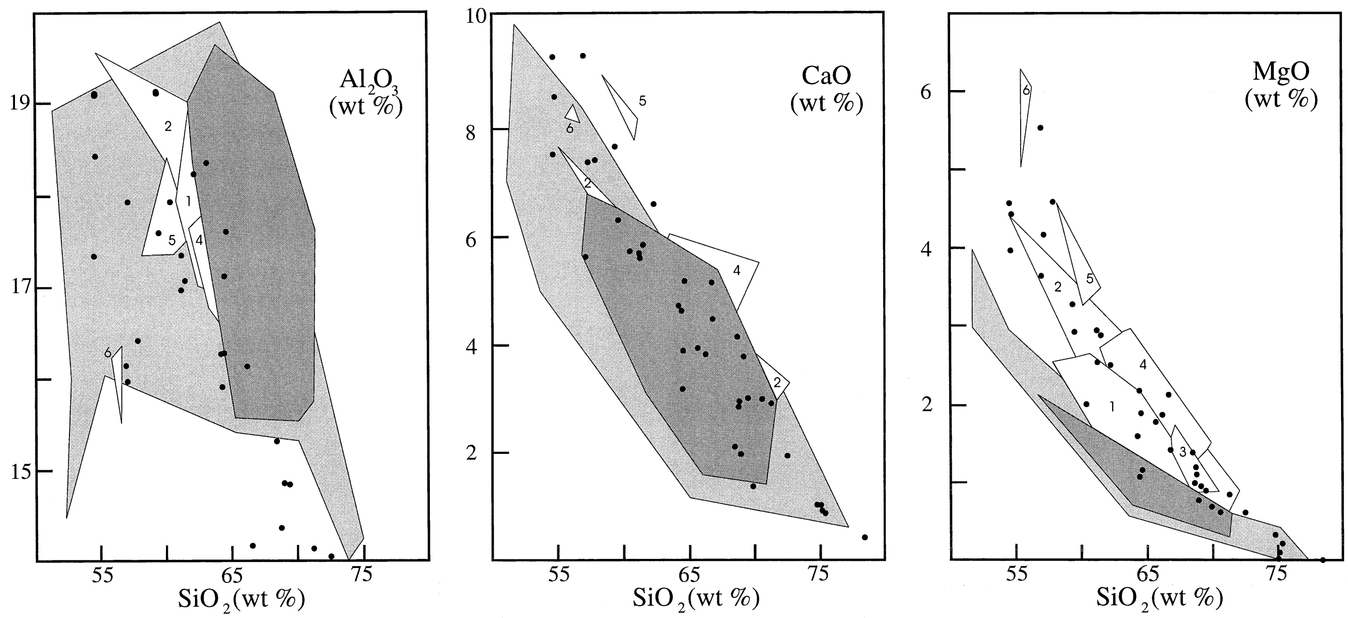

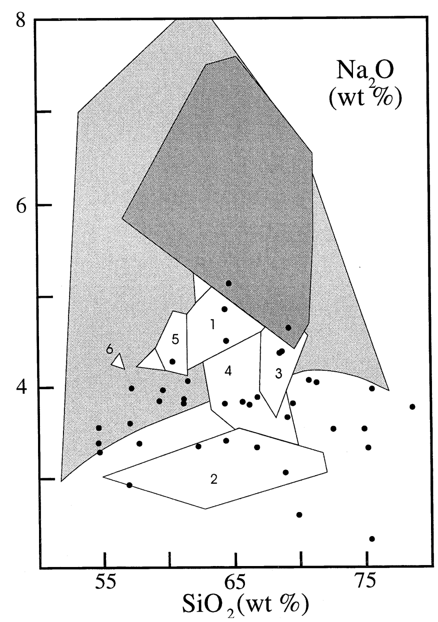

Fig. 10 Comparison of experimentally produced melt compositions (*stipple*) with those of the western Palmer Land granites (*filled circles*), and suggested adakites. [The experimental data shown are: *dark stipple* Rapp et al. (1991) and Sen and Dunn (1994), *light stipple* (Rapp and Watson (1995)]. Figure modified after Sen and Dunn (1994). Suggested adakite compositions are: *1* Mt. St. Helens (Smith and Leeman 1987), *2* Skagway tonalite (Barker et al. 1986), *3* La Yeguada Volcanic Complex (Defant et al. 1991), *4* Mindanao, Philippines (Sajona et al. 1993), *5* Isla Cook, Patagonia (Puig et al. 1984), *6* Baja, California (Rogers et al. 1985)

temporal variations in Sr/Y, which we would expect if the granite magmas were generated in response to the subduction of young ocean lithosphere during the Mesozoic. Moreover, the *P–T* model of Drummond and Defant (1990) suggests that the adakitic arc should lie outboard of the main calc-alkaline plutonic/volcanic arc, whereas the generation of both granite types in western Palmer Land overlaps in space and time. The primary source for LILE-enriched and HFSE-depleted arc magmas, such as those in western Palmer Land, is generally considered to be mantle wedge peridotite that has been metasomatised by H_2O- and/or CO_2-rich fluids derived from dehydrating subducting ocean lithosphere (e.g. Saunders et al. 1980; Tatsumi et al. 1986; McInnes and Cameron 1994; Stolper and Newman 1994). If adakitic melt was a common, and significant, mantle wedge component then we would expect Archean TTG-like magmas to be present in all arcs, which is clearly not the case (e.g. Martin 1986; Drummond and Defant 1990). Adakitic melt is possibly only an important mantle wedge component where the subducting slab at the trench is young (< 25 Ma?) and capable of melting significantly. We conclude that the WPLG were probably not generated from melting oceanic lithosphere.

The mantle wedge

Geochemical similarities between basaltic and granitic intrusions in western Palmer Land (e.g. Figs. 4 and 6) suggest that the WPLG may be differentiates of mantle wedge magmas. The low MgO, Ni and Cr contents of

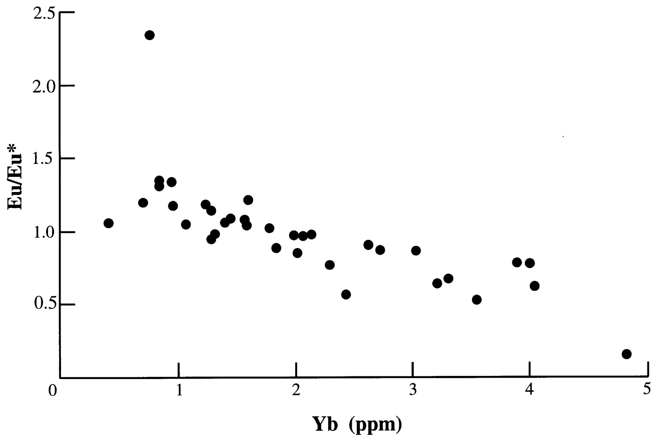

Fig. 11 Plot of Eu/Eu* versus Yb for the western Palmer Land granites

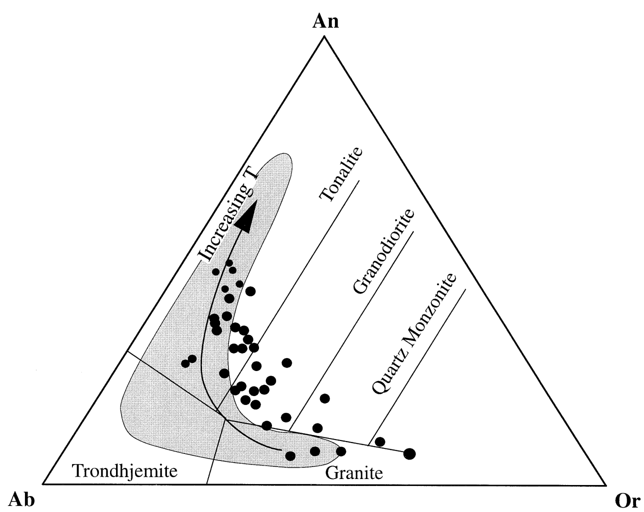

Fig. 12 Normative albite (*Ab*)- anorthite (*An*)- orthoclase (*Or*) ternary plot contrasting the compositions of the western Palmer Land granites with those of experimental melts (after Sen and Dunn 1994). Experimental melt compositions (*stipple*) are from Rapp et al. (1991), Wolf and Wyllie (1993), Rushmer (1991). *Arrow* shows compositional variation with increasing temperature

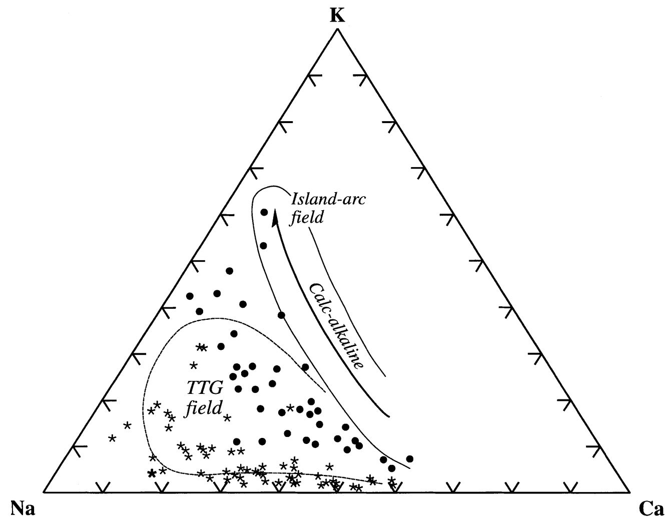

Fig. 13 Atomic Ca-Na-K ternary plot. TTG field encompasses all Archean trondhjemites, tonalites and granodiorites believed to be partial melt products of metabasalt (Drummond and Defant 1990). Calc-alkaline field and fractionation trend is from Nockolds and Allen (1953). [Data plotted are: *filled circles* western Palmer Land granites, *stars* experimental melt compositions of Rapp et al. (1991) and Rapp and Watson (1995)]. Figure modified from Defant and Drummond (1993)

the WPLG would require such mantle magmas to have fractionated olivine and clinopyroxene, whilst their high and variable Sr/Y and La/Yb, but relatively low Y and HREE content and K/Rb would require hornblende fractionation. The trajectory in Fig. 6, particularly the occurrence of low-$\varepsilon Nd_{(t)}$ and high-$\varepsilon Sr_{(t)}$ plutons, would also require such mantle melts to have assimilated continental crust, such as Triassic or older gneiss.

Crustal contamination of mantle melts may occur by several mechanisms, including assimilation concomitant with fractional crystallisation (AFC; DePaolo 1981). Advantageous selection of contaminant and parent magma compositions, assimilation rates, and bulk distribution coefficients allows us to reproduce the Sr and Nd isotope compositions of the WPLG by AFC. However, we shall demonstrate that it is difficult to reconcile trace element compositions of the WPLG by AFC alone.

We constructed AFC models to determine whether the low-Y and -HREE contents and high La/Yb and Sr/Y of the WPLG could be derived from mafic dyke magmas in the region (Table 1). A high assimilation: crystallisation rate of 0.7, applicable to lower crustal regions, where the crust is hot and easy to consume, was used (DePaolo 1981). The initial magma composition modelled in the calculations was that of a Y- and HREE-poor, primitive, basaltic dyke (R.5717.3; Table 1). This composition was chosen to enhance the generation of low-Y + HREE granite magmas in the calculations. It has a rather low Y (16 ppm) and Yb (1.6 ppm) content, as the average Y content of 67 mafic dykes is ca. 25 ppm and the average Yb content of 33 mafic dykes is ca. 2.7 ppm (C.D. Wareham unpublished data). Because there is little exposed basement in the Antarctic Peninsula for which compositional data is available, the lower crust compositions of Taylor and McLennan (1995) were used in Fig. 14, and Target Hill (Graham Land) gneiss (Milne 1990) in Figs. 9 and 15.

A selection of AFC trajectories for hornblende-, clinopyroxene- and garnet-bearing assemblages are shown in Figs. 9, 14 and 15. Garnet is included as a fractionating phase because of its stability at lower crustal pressures (Huang and Wyllie 1986).

Plagioclase fractionation was not modelled because its presence would lower the bulk partition coefficients of the HREE and Y, and because its removal would deplete the model magma in Sr.

High degrees of hornblende fractionation could produce the Sr/Y of the WPLG, although this would be at

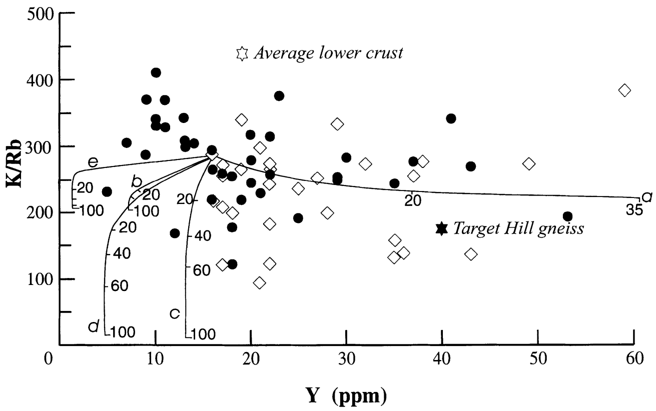

Fig. 14 Plot of K/Rb versus Y for western Palmer Land granites (*filled circles*), basaltic dykes (*diamonds*), average lower crust of Taylor and McLennan (1995) and Target Hill gneiss (Milne 1990). AFC trajectories are for clinopyroxene (*a*), 0.7 dinopyroxene 0.3 garnet (*b*), hornblende (*c*) 0.7 hornblende 0.3 garnet (*d*), garnet (*e*). AFC modelled using an assimilation:crystallisation of ratio 0.7 and an initial magma composition of R.5717.3 (Table 1). Contaminant has 40 ppm Y, 180 ppm Rb and 32000 ppm K. Partition coefficients as per Table 2

the expense of little variation in Y content (Fig. 9). Moreover, this would also produce peraluminous magmas, whereas the WPLG are predominantly metaluminous. In contrast, clinopyroxene fractionation has little effect on Sr/Y but could easily produce a wide range of Y concentrations. Because garnet fractionation rapidly depletes magmas in Y without affecting their Sr content, magmas with a range of Y and Sr/Y can result from

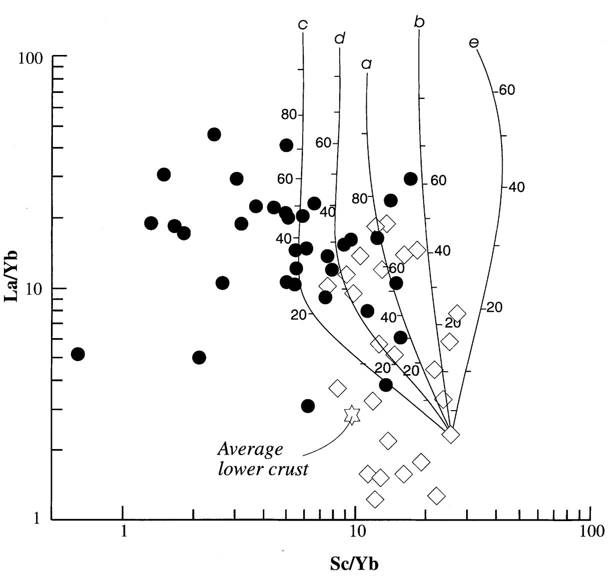

Fig. 15 Plot of Sc/Yb versus La/Yb for western Palmer Land granites (*filled circles*) basaltic dykes (*diamonds*) and average lower crust of Taylor and McLennan (1995). AFC trajectories are for clinopyroxene (*a*), 0.7 clinopyroxene 0.3 garnet (*b*), hornblende (*c*) 0.7 hornblende 0.3 garnet (*d*), garnet (*e*). AFC modelled using an assimilation:crystallisation ratio of 0.7 and an initial magma composition of R.5717.3 (Table 1). Contaminant has 11 ppm La, 2.2 ppm Yb, and 36 ppm Sc. Partition coefficients as per Table 2

fractionation of hornblende + garnet and clinopyroxene + garnet (Fig. 9).

It is also difficult to produce the low-Y WPLG by AFC processes because potential parent magmas and crustal contaminants in the region are Y-rich (Fig. 14): the average Y content of mafic dyke magmas is ca. 25 ppm, Target Hill gneiss has an average Y content of ca. 30 ppm (Milne 1990) and eastern Palmer Land gneisses have > 40 ppm Y (Wever et al. 1995). Low Y (+HREE) magmas could in theory be generated if garnet was a major fractionating phase, although the effects of this on Sc/Yb will be discussed. Moreover, the generation of high K/Rb granite magmas by reasonable AFC models is not possible (Fig. 14).

High La/Yb WPLG can be generated from low La/Yb parental magmas by high degrees of hornblende and clinopyroxene fractionation, although concomitant fractionation of garnet would produce high La/Yb residual magmas more easily (Fig. 15). However, clinopyroxene fractionation alone produces little variation in Sc/Yb, whilst garnet fractionation drives Sc/Yb towards higher values than those of the WPLG. It is only possible to generate the high La/Yb and low Sc/Yb granite magmas from the lowest Sc/Yb mafic dyke magmas if they fractionate hornblende.

It is evident that generating the complete range of Y, Sr/Y, K/Rb, La/Yb, and Sc/Yb compositions of the WPLG by AFC alone would necessitate the involvement of more than one parent magma and/or multiple crystallisation and assimilation events involving high degrees of hornblende and clinopyroxene (± garnet) fractionation.

An alternative, and perhaps complementary, crustal contamination scenario to AFC is that of mantle wedge magmas mixing with partial melts of continental crust. Hildreth and Moorbath (1988) suggested that volcanic rocks in Chile with adakitic characteristics were produced by such a process. They hypothesised the existence of lower crustal zones of mixing, assimilation, storage and homogenisation of mantle wedge magmas and crustal melts. The low Y + HREE content of the volcanic rocks requires that the crustal melts were Y + HREE poor, implying that they were generated within the garnet stability field, at deep crustal levels > ca. 36 km (Rapp and Watson 1995). The εNd of these volcanic rocks varies inversely with their La/Yb and reflects the proportion of crustal partial melt present (cf. Feeley and Davidson 1994; Feeley and Hacker 1995).

The high Y + HREE content of mafic dyke magmas in western Palmer Land relative to the WPLG suggests that the granites would need to contain a significant component of crustal partial melt. Moreover, the high Y + HREE content of basement gneiss in the region would also require the partial melting to occur at depths appropriate to the garnet stability field (cf. Hildreth and Moorbath 1988). However, unlike Andean adakitic volcanic rocks, there is no clear correlation between the εNd and La/Yb of the WPLG. Thus, the WPLG are unlikely to be just mixtures of mantle wedge magmas and partial melts of Triassic and older continental crust (cf. Fig. 6).

Thick (> 10 km) sill-like bodies of mafic magma are thought to be intruded (underplated) at, or slightly above, the base of the crust in many arcs (Hamilton 1995; Suyehiro et al. 1996) and would lead to elevated lower crustal temperatures and partial melting (cf. Atherton and Petford 1993). Consequently, juvenile basaltic crust must be considered as an additional magma source.

Basaltic lower crust

Field and experimental studies indicate that amphibolite and basaltic-amphibolite can produce significant volumes of partial melt at lower crustal temperatures and pressures, particularly in arcs where mafic magmatism sustains high heat flow (e.g. Rushmer 1991). Atherton and Petford (1993) suggested that adakitic volcanic rocks can be produced solely from partial melting of juvenile (i.e. warm), garnet-bearing, basaltic lower crust. The main difference between partial melting reactions in basaltic lower crust and subducting oceanic lithosphere is protolith composition. Mafic magmas that underplate arc crust are likely to be equivalents of western Palmer Land mafic dykes and gabbro (i.e. predominantly calc-alkaline basalt and basaltic andesite) not NMORB. Partial melts of this material will have different compositions to low-K tholeiites, the starting compositions used in most experimental studies (cf. Figs. 10, 12 and 13). For instance, mafic arc magmas will undoubtedly produce higher Sr/Y and La/Yb partial melts than NMORB when fused, as they are relatively enriched in LILEs and LREEs, but depleted in many HFSEs and HREEs (e.g. Fig. 4 and Table 1). Moreover, arc crust is susceptible to fluxing by slab-derived fluids and this will also influence the composition any partial melt (Winther 1996). Consequently, the WPLG may have compositions atypical of partial melts of NMORB, but they may be typical of melting calc-alkaline basaltic and andesitic underplate. Nevertheless, as basaltic magmatism in western Palmer Land has higher Y + HREE contents than many WPLG, any partial melting of underplate would need to occur at deep (> 36 km) crustal levels, where garnet is stable.

Discussion

Hildreth and Moorbath (1988) and Atherton and Petford (1993) concluded that adakitic volcanic rocks were produced when mafic arc magmas melted Andean crust. But, whereas Hildreth and Moorbath invoked mixing between mantle magmas and crustal melts, Atherton and Petford suggested that volcanic rocks of the Cordillera Blanca are predominantly (entirely?) crustal melts. Melting of arc crust is inevitable in subduction settings, because heat is advected from the mantle to the crust by mafic magmas. Both models require crustal melting to occur at depths ≥36 km, such that garnet is stable. However, extension in the overriding plate is the norm in arcs (Hamilton 1995) and extensional features controlled the emplacement of many granite *s.l.* and gabbro plutons in western Palmer Land (e.g. Storey et al. 1996; Vaughan and Millar 1996). Thus, the extending Palmer Land Crust must have been thicker than normal arc crust for garnet to have been stable during crustal melting (cf. Taylor and McLennan 1985).

Crustal thickening

The intrusion of mafic magmas into the lower crust (underplating) is a common phenomenon in arcs (Hamilton 1995). Suyehiro et al. (1996) suggested that underplating and intraplating of mafic magma into extending arc crust compensates for tectonic thinning. We suggest that underplating of mafic magmas also resulted in crustal thickening in Palmer Land. Outcrop of Lower Cretaceous gabbro in western Palmer Land coincides with prominent regional magnetic anomalies, part of a belt of positive magnetic anomalies along the west coast of the Antarctic Peninsula (Renner et al. 1985; Maslanyj et al. 1990; Johnson and Smith 1992). This spatial association suggests that mafic additions to the crust may have been significant during the Cretaceous. The presence of a ca. 15 km thick section of flat-lying to shallowly dipping, high velocity (v_p ca. 7.1 km s^{-1}), lower crustal seismic reflectors above the Moho elsewhere in the Antarctic Peninsula (Conway 1992) is consistent with basaltic underplating of the arc.

Granite magma sources

Many WPLG have similar chemical compositions to partial melts of basaltic material at 8 to 30 kbar which, with their relatively high $\varepsilon Nd_{(t)}$ (Fig. 6) and the evidence for magmatic crustal thickening, suggests that they may be partial melts of juvenile basaltic underplate (cf. Atherton and Petford 1993). Nevertheless, the plutons have characteristics that suggest additional mantle and crustal sources were involved in their genesis. Trace element compositions, evidence of widespread mixing and mingling of mafic and granitic magmas and MgO and Na_2O relationships suggest that many, if not all, WPLG contain a component of mantle melt, in accord with their generation above a subduction zone producing mafic magmas. Conversely, the occurrence of low-$\varepsilon Nd_{(t)}$ and high-$\varepsilon Sr_{(t)}$ plutons and the trajectory in Fig. 6 suggest that perhaps all except the highest $\varepsilon Nd_{(t)}$ plutons contain a component of Pre-Triassic–Triassic crust.

We prefer a model akin to that of Hildreth and Moorbath (1988) for generating the granite *s.l.* magmas in western Palmer Land. Mafic arc magmas were produced following the hydration of mantle wedge peridotite by fluids from the subducting slab. These magmas were subsequently contaminated by arc crust, probably during deep crustal fractionation of olivine, pyroxene and amphibole. Slab-melt characteristics, such as low Y + HREE, were acquired by magmas which mixed with partial melts of garnet-bearing arc crust. The Nd and Sr isotope data are consistent with the involvement of juvenile basaltic crust (underplate) and Triassic–Pre-Triassic basement. The occurrence of contemporaneous adakitic and "normal" calc-alkaline WPLG suggests that not all the crust involved in their genesis was garnet bearing. Isotope and trace element data are compatible with partial melt of juvenile basaltic underplate being a dominant component of some WPLG, in keeping with their overall tectono-magmatic setting (cf. Atherton and Petford 1993). Assimilation and fractional crystallisation cannot be ruled out as contributory processes in generating the trace element compositions of the WPLG, particularly at shallow crustal levels where plagioclase was a fractionating phase (cf. Fig. 9). Nevertheless, because the WPLG have a wide range of trace element compositions (e.g. Fig. 14), AFC is considered to be supplementary to magma mixing, assimilation, storage and homogenisation.

Lower crustal zones of magma mixing, assimilation, storage and homogenisation are probably common to all arcs, because mafic magmatism, such as by underplating, and high heat flow are inevitable. However, magmas with Archean TTG and adakite characteristics will only be generated where the crust is thick enough for garnet to be stable during crustal melting. The production of crust that is both thick and warm enough to melt is most likely in regions that have long histories of subduction magmatism, where the crust can be thickened magmatically and tectonically and high heat flow sustained for long periods. Mixing between mantle and crustal melts is probably the norm in arcs, but in exceptional circumstances purely crustal melts may be produced (Atherton and Petford 1993). The occurrence of adakitic plutonic and volcanic rocks along the proto-Pacific margin of Gondwana, in the Antarctic Peninsula, New Zealand and South America, is testament to the effects that prolonged subduction can have on the character of the magmatism.

Crustal growth

The Nd isotope compositions of granite magmas in western Palmer Land increased by ca. 10 ε units between the Triassic and Tertiary (Fig. 7). Such temporal increases in $\varepsilon Nd_{(t)}$ within a magmatic suite are generally considered to be indicative of crustal growth (Nelson and DePaolo 1984; DePaolo et al. 1991; Johnson 1993). However, partial melts of juvenile basaltic lower crust are isotopically indistinguishable from mantle wedge magmas and we are unable to ascertain their relative roles in producing the $\varepsilon Nd_{(t)}$ variation. All we can say is that the role of Triassic and older continental crust waned with time. The slight (just larger than analytical error) decrease in $^{207}Pb/^{204}Pb_{(t)}$ with pluton age concomitant with increasing $\varepsilon Nd_{(t)}$ and decreasing $\varepsilon Sr_{(t)}$ supports this. Shifts in Pb isotope composition are smaller in magnitude than those for Sr and Nd for two main reasons. Firstly, mantle-derived mafic magmas are generally poorer in Pb than average crustal rocks and their Pb isotope compositions are consequently dominated by that of any crust they assimilate. Secondly, Pb is more soluble in hydrous fluids than Sr and Nd, making the Pb isotope composition of the crust more susceptible to homogenisation by hydrothermal circulation (cf. McCulloch and Woodhead 1993). Shifts in the total crustal Pb isotope composition of arc crust are most likely to occur by repeated injection of mafic magmas, such as by underplating and intraplating.

Ellam and Hawkesworth (1988) noted that the net flux of material into the crust in recent arcs is basaltic, but that continental crust is broadly andesitic. Partial melts of garnet- and amphibole-bearing lower crust are more LREE-enriched than both basaltic melts they may mix with and basaltic intrusions previously accreted to the lower crust. Crustal assimilation and magma mixing, storage and homogenisation processes (Moorbath and Hildreth 1988) will generate broadly LREE- and LILE-enriched, andesitic–granitic, continental crust in arc environments, where the net flux of magma is predominantly basalitc. The garnet-rich amphibolite and pyroxenite residues formed by high *P–T* partial melting reactions are denser than average plagioclase-bearing lower continental crust and the underlying mantle and may detach and sink into the convecting asthenosphere (Kay and Kay 1991). This process will drive initially mafic and HREE-rich arc crustal compositions towards more andesitic, LREE-enriched compositions. Moreover, little net growth in crustal mass would have resulted, contrary to that indicated by isotopic analysis of upper crustal granites and volcanic rocks, although structural data suggest that emplacement of granite resulted in net crustal growth (Vaughan and Millar 1996).

Conclusions

1. Subduction generated basaltic magmas contributed to crustal thickening by underplating in western Palmer Land. This aided the production of arc crust that was thick and hot enough to melt while garnet was stable as a lower crustal phase.

2. Juvenile basaltic underplate and Triassic–Pre-Triassic basement was partially melted by subsequent influxes of basaltic magma. Mixing between these partial melts and contemporaneous mantle melts in deep crustal zones of mixing, assimilation, storage and homogenisation produced granite magmas with compositional characteristics that are usually associated with Archean TTG suites.

3. Temporal variations in the Sr, Nd and Pb isotope compositions of the WPLG are consistent with lower crustal hybridisation during arc magmatism. The relationships we observe between εNd and stratigraphic age

are consistent with the melting of progressively younger underplate, and/or mixing of an increased component of basaltic melt. The isotope data reflect the addition of mantle-derived material to the crust. However, if garnet-bearing lower crust was to delaminate then, contrary to what the isotope data would lead us to believe, little net growth in crustal mass would have occurred. Nonetheless, partial melts extracted from juvenile underplate and incorporated at higher crustal levels would have been removed from the ''delamination zone'' and structural evidence suggests arc crustal growth by magmatism during extension.

Acknowledgements The authors would like to thank the field and air operations staff at Rothera Base for logistical support, and Alistair Taylor and Paul Farmer for their field assistance. Earlier versions of the manuscript benefited from comments by Drs. Phil Leat, Jane Scarrow and Bryan Storey. Reviews by Drs. Nick Petford and Andy Saunders led to significant improvements in the manuscript.

References

Alabaster T, Storey BC (1990) Modified Gulf of California model for South Georgia, north Scotia Ridge, and implications for the Rocas Verdes back-arc basin, southern Andes, Geology 18: 497–500

Arth JG (1979) Some trace elements in trondhjemites – their implications to magma genesis and palaeotectonic setting. In: Barker F (ed) Trondhjemites, dacites, and related rocks. Elsevier, New York, pp 123–132

Atherton MP, Petford N (1993) Generation of sodium-rich magmas from newly underplated basaltic crust. Nature 362: 144–146

Barker PF (1982) The Cenozoic subduction history of the Pacific margin of the Antarctic Peninsula: ridge crest-trench interactions. J Geol Soc London 139: 787–801

Barker F, Arth JG, Stern TW (1986) Evolution of the Coast batholith along the Skagway Traverse, Alaska and British Columbia. Am Mineral 71: 632–643

Barnes CG, Petersen SW, Kistler RW, Murray R, Kays MA (1996) Source and tectonic implications of tonalite–trondhjemite magmatism in the Klamath Mountains. Contrib Mineral Petrol 123: 40–60

Catanzaro EJ, Murphy TJ, Shields WR, Garner EL (1968) Absolute isotopic abundance ratios of common, equal atom, and radiogenic lead isotope standards. J Res Nat Bur Stand 72A: 261–267

Conway AM (1992) Crustal structure off the Antarctic Peninsula south west of Anvers Island (unpublished). PhD thesis, Birmingham Univ

Davies JH, Stevenson DJ (1992) Physical model of source region of subduction zone volcanics. J Geophys Res 97: 2037–2070

Defant MJ, Drummond MS (1990) Derivation of some modern arc magmas by melting of young subducted lithosphere. Nature 347: 662–665

Defant MJ, Clark LF, Stewart RH, Drummond MS, de Boer JZ, Maury RC, Bellon H, Jackson TE, Restrepo JF (1991) Andesite and dacite genesis via contrasting processes: the geology and geochemistry of E1 Valle Volcano, Panama. Contrib Mineral Petrol 106: 309–324

DePaolo DJ (1981) Trace element and isotopic effects of combined wall-rock assimilation and fractional crystallization. Earth Planet Sci Lett 53: 189–203

DePaolo DJ, Linn AM, Schubert G (1991) The continental crustal age distribution: methods of determining mantle separation ages from Sm-Nd isotope data and applications to the southwestern United States. J Geophys Res 96: 2071–2088

Drummond MS, Defant MJ (1990) A model for trondhjemite–tonalite–dacite genesis and crustal growth via slab melting: Archean to modern comparisons. J Geophys Res 95: 21503–21521

Ellam RM, Hawkesworth CJ (1988) Is average continental crust generated at subduction zones? Geology 16: 314–317

Feeley TC, Davidson JP (1994) Petrology of the calc-alkaline lavas at Volcán Ollagüe and the origin of compositional diversity at central Andean stratovolcanoes. J Petrol 35: 1295–1340

Feeley TC, Hacker MD (1995) Intracrustal derivation of Na-rich andesite and dacite magmas: an example from Volcán Ollagüe, Andean Central Volcanic Zone. J Geol 103: 213–225

Floyd PA (1985) Petrology and Geochemistry of oceanic intraplate sheet-flow basalts, Naru Basin DSDP Leg 89. In: Moberly R et al (eds) Initial Rep DSDP 89, pp 471–497

Gariépy C, Allègre CJ (1985) The lead isotope geochemistry and geochronology of late-kinematic intrusives from the Abitibi greenstone belt, and the implications for late Archaean crustal evolution. Geochim Cosmochim Acta 49: 2371–2383

Green TH (1994) Experimental studies for trace-element partitioning applicable to igneous petrogenesis – Sedona 16 years later. Chem Geol 117: 1–36

Hamilton WB (1995) Subduction systems and magmatism. Geol Soc London Spec Publ 81: 3–28

Harrison SM (1989) Aspects of magmatism and metamorphism within a magmatic arc: evidence from north-western Palmer Land, Antarctic Peninsula (unpublished). PhD thesis, Counc Nat Acad Awards

Harrison SM, Piercy BA (1990) The evolution of the Antarctic Peninsula magmatic arc: evidence from northwestern Palmer Land. Geol Soc Am Spec Publ 241: 9–25

Hauri EH, Wagner TP, Grove TL (1994) Experimental and natural partitioning of Th, U, Pb and other trace elements between garnet, clinopyroxene and basaltic melts. Chem Geol 117: 149–166

Hawkesworth CJ, Clarke E (1994) Partial melting in the lower crust: new constraints on crustal contamination processes in the central Andes. In: Reutter KJ, Scheuber E, Wigger PJ (eds) Tectonics of the Southern Central Andes. Springer Verlag, Berlin Heidelberg New York, pp 93–101

Helz RT (1976) Phase relations of basalts in their melting ranges at P_{H_2O} = 5kbar. II. Melt compositions. J Petrol 17: 139–193

Henderson P (1982) Inorganic geochemistry. Pergamon Press, Oxford

Hildreth W, Moorbath S (1988) Crustal contributions to arc magmatism in the Andes of central Chile. Contrib Mineral Petrol 98: 455–489

Hochstaedter AG, Kepezhinskas PK, Defant MJ, Drummond MS, Bellon H (1994) On the tectonic significance of arc volcanism in northern Kamchatka. J Geol 102: 639–654

Hole MJ (1986) Time controlled geochemistry of igneous rocks of the Antarctic Peninsula (unpublished). PhD thesis, Bedford College, Univ London

Hole MJ, Pankhurst RJ, Saunders AD (1991) Geochemical evolution of the Antarctic Peninsula magmatic arc: the importance of mantle-crust interactions during granitoid genesis. In: Thomson MRA, Crame JA, Thomson JW (eds) Geological evolution of Antarctica. Cambridge University Press, Cambridge, pp 369–374

Hole MJ, Kempton PD, Millar IL (1993) Trace-element and isotopic characteristics of small-degree melts of the asthenosphere: evidence from the alkalic basalts of the Antarctic Peninsula. Chem Geol 109: 51–68

Huang WL, Wyllie PJ (1986) Phase relationships of gabbro-tonalite-granite-water at 15 kbar with applications to differentiation and anatexis. Am Mineral 71: 301–316

Johnson AC, Smith AM (1992) New aeromagnetic map of West Antarctica (Weddell Sea sector): introduction to important features. In: Yoshida Y, Kaminuma K, Shiraishi K (eds) Recent progress in Antarctic science. Tokyo, Terrapub, pp 555–562

Johnson CM (1993) Mesozoic and Cenozoic contributions to crustal growth in the southwestern United States. Earth Planet Sci Lett 118: 75–89

Kay RW (1978) Aleutian magnesian andesites: melts from subducted Pacific ocean crust. J Volcanol Geothermal Res 4: 497–522

Kay RW, Kay SM (1991) Creation and destruction of lower continental crust. Geol Rundsch 80: 259–278

Kay SM, Ramos VA, Marquez M (1993) Evidence in Cerro Pampa volcanic rocks for slab-melting prior to ridge-trench collision in southern South America. J Geol 101: 703–714

Kepezhinskas PK, Defant MJ, Drummond MS (1995) Na metasomatism in the island-arc mantle by slab melt-peridotite interaction: evidence from mantle xenoliths in the North Kamchatka Arc. J Petrol 36: 1505–1527

Larter R, Barker PB (1991) Effects of ridge-crest trench interaction on Antarctic-Phoenix spreading: forces on a younger subducting plate. J Geophys Res 96: 19583–19607

Leat PT, Scarrow JH, Millar I (1995) On the Antarctic Peninsula batholith. Geol Mag 132: 399–412

Le Maitre RW (1989) A classification scheme of igneous rocks and a glossary of terms. Blackwell Scientific Press, Oxford

Loske W, Miller H (1991) Rb-Sr and U-Pb geochronology of basement xenoliths at Cape Dubouzet, Antarctic Peninsula (abstract). In: Int Symp Antarct Earth Sci. Nat Inst Polar Res, Japan, pp 374–379

Martin H (1986) Effect of steeper Archean geothermal gradient on geochemistry of subduction zone magmas. Geology 14: 753–756

Martin H (1987) Petrogenesis of Archean trondhjemites, tonalites, and granodiorites from eastern Finland: major and trace element geochemistry. J Petrol 28: 921–953

Maslanyj MP, Garrett SW, Johnson AC, Renner RGB, Smith AM (1990) Aeromagnetic anomaly map of West Antarctica (Weddell Sea sector). BAS GEOMAP Series, Sheet 2, 1:2,500,000, with supplementary text. Cambridge, British Antarctic Survey

Maury RC, Defant MJ, Joron JL (1992) Metasomatism of the sub-arc mantle inferred from trace elements in Philippine xenoliths. Nature 360: 661–663

McCarron JJ (1995) Evolution and tectonic implications of late Cretaceous–early Tertiary fore-arc magmatism: Alexander Island, Antarctica (unpublished) PhD thesis, Univ Cambridge

McCulloch MT, Woodhead JD (1993) Lead isotope evidence for deep crustal-scale fluid transport during granite petrogenesis. Geochim Cosmochim Acta 57: 659–674

McInnes BIA, Cameron EM (1994) Carbonated, alkaline metasomatic melts from a sub-arc environment: mantle wedge samples from the Tabar-Lihir-Tanga-Feni arc, Papua New Guinea. Earth Planet Sci Lett 122: 125–141

Miller CF, Barton MD (1990) Phanerozoic plutonism in the Cordilleran Interior, USA. Geol Soc Am Spec Publ 241: 213–231

Milane AJ (1990) The pre-Mesozoic geological evolution of Graham Land, Antarctica (unpublished). PhD thesis, Open Univ

Milane AJ, Millar IL (1989) The significance of mid-Palaeozoic basement in Graham Land, Antarctic Peninsula. J Geol Soc London 146: 207–210

Molner P, England P (1995) Temperatures in zones of steady-state underthrusting of young oceanic lithosphere. Earth Planet Sci Lett 131: 57–70

Moyes AB (1986) The Jinks Island complex – magma mixing in a high-level intrusion from the Biscoe Islands, Antarctic Peninsula. Br Antarct Surv Bull 70: 55–69

Muir RJ, Weaver SD, Bradshaw JD, Eby GN, Evans JA (1995) The Cretaceous Separation Point batholith, New Zealand: granitoid magmas formed by melting of mafic lithosphere. J Geol Soc London 152: 689–702

Nakamura N (1974) Determination of REE, Ba, Fe, Mg, Na and K in carbonaceous and ordinary chondrites. Geochim Cosmochim Acta 38: 757–775

Nelson BK, DePaolo DJ (1984) 1,700 Ma greenstone successions in southwestern North America and evolution of Proterozoic mantle. Nature 312: 143–146

Nichols GT, Wyllie PJ, Stern CR (1994) Subduction zone melting of pelagic sediments constrained by melting experiments. Nature 371: 785–788

Nockolds SR, Allen R (1953) The geochemistry of some igneous rock series. Geochim Cosmochim Acta 4: 105–142

Pankhurst RJ (1982) Rb-Sr geochronology of Graham Land, Antarctica. J Geol Soc London 139: 701–711

Pankhurst RJ (1990) The Paleozoic and Andean magmatic arcs of West Antarctica and southern South America. Geol Soc Am Spec Publ 241: 1–7

Pankhurst RJ, Rapela CR (1995) Production of Jurassic rhyolite by anatexis of the lower crust of Patagonia. Earth Planet Sci Lett 134: 23–36

Pankhurst RJ, Hole MJ, Brook M (1988) Isotope evidence for the origin of Andean granites. Philos Trans R Soc Edinburgh 79: 123–133

Paterson SR, Vernon RH, Tobisch OT (1989) A review of criteria for the identification of magmatic and tectonic foliations in granitoids. J Struct Geol 11: 349–363

Peacock SM, Rushmer T, Thompson AB (1994) Partial melting of subducting oceanic crust. Earth Planet Sci Lett 121: 227–244

Peccerillo A, Taylor SR (1976) Geochemistry of Eocene calc-alkaline volcanic rocks from the Kastamonu area, northern Turkey. Contrib Mineral Petrol 58: 63–81

Pichowiak S, Buchelt M, Damm K-W (1990) Magmatic activity and tectonic setting of the early stages of the Andean cycle in northern Chile. Geol Soc Am Spec Publ 241: 127–144

Potts PJ (1987) A handbook of silicate analysis. Blackie, London

Puig A, Herve E, Suarez M, Saunders AD (1984) Calc-alkaline and alkaline Miocene and calc-alkaline Recent volcanism in the southernmost Patagonian Cordillera, Chile. J Volcanol Geothermal Res 20: 149–163

Rapp RP, Shimizu N (1995) Partitioning of REEs, Ti, Sr, Y, Cr and Zr between tonalitic-trondhjemitic-granitic melts and eclogite residue at 1–11 GPa: ion microprobe analyses at natural abundance levels. EOS Trans Am Geophys Union 76: 296

Rapp RP, Watson EB (1995) Dehydration melting of metabasalt at 8–32 kbar: implications for continental growth and crust-mantle recycling. J Petrol 36: 891–932

Rapp RP, Watson EB, Miller CF (1991) Partial melting of amphibolite/eclogite and the origin of Archean trondhjemites and tonalites. Precambrian Res 51: 1–25

Renner RGB, Sturgeon LJS, Garrett SW (1985) Reconnaissance gravity and aeromagnetic surveys of the Antarctic Peninsula. Br Antarct Surv Sci Rep 110

Rex DC (1976) Geochronology in relation to the stratigraphy of the Antarctic Peninsula. Br Antarct Surv Bull 43: 49–58

Richter FM (1988) A major change in the thermal state of the earth at the Archean-Proterozoic boundary: consequences for the nature and preservation of continental lithosphere. J Petrol Spec Lithospheric Issue: 39–52

Rogers G, Saunders AD, Terrell DJ, Verma SP, Marriner GF (1985) Geochemistry of Holocene volcanic rocks associated with ridge subduction in Baja, California, Mexico. Nature 315: 389–392

Rushmer T (1991) Partial melting of two amphibolites: contrasting experimental results under fluid-absent conditions. Contrib Mineral Petrol 107: 41–59

Sajona FG, Maury RC, Bellon H, Cotten J, Defant MJ, Pubellier M (1993) Initiation of subduction and the generation of slab melts in western and eastern Mindanao, Philippines. Geology 21: 1007–1010

Saunders AD, Tarney JT, Weaver SD (1980) Transverse geochemical variations across the Antarctic Peninsula: implications for the genesis of calc-alkaline magmas. Earth Planet Sci Lett 46: 344–360

Schiano P, Clocchiatti R, Shimizu N, Maury RC, Jochum KP, Hofmann AW (1995) Hydrous, silica-rich melts in the sub-arc mantle and their relationships with erupted arc lavas. Nature 377: 595–600

Sen C, Dunn T (1994) Dehydration melting of basaltic composition amphibolite at 15 and 3 GPa: implications for the origin of adakites. Contrib Mineral Petrol 117: 394–409

Smith DR, Leeman WP (1987) Petrogenesis of Mount St. Helens dacitic magmas. J Geophys Res 92: 10313–10334

Stern RA, Hanson GN (1900) Archean high-Mg granodiorite: a derivative of light rare earth element-enriched monzodiorite of mantle origin. J Petrol 32: 201–238

Stolper E, Newman S (1994) The role of water in the petrogenesis of Mariana trough magmas. Earth Planet Sci Lett 121: 293–325

Storey BC, Alabaster T, Hole MJ, Pankhurst RJ, Wever HE (1992) Role of subduction-plate boundary forces during the initial stages of Gondwana break-up: evidence from the proto-Pacific margin of Antarctica. Geol Soc London Spec Publ 68: 149–164

Storey BC, Vaughan APM, Millar IL (1996) Geodynamic evolution of the Antarctic Peninsula during Mesozoic times and its bearing on Weddell Sea History. Geol Soc London Spec Publ 108: 87–103

Suárez M (1976) Plate tectonic model for southern Antarctic Peninsula and its relation to southern Andes. Geology 4: 211–214

Sun S-s; McDonough WF (1989) Chemical and isotopic systematics of oceanic basalts: implications for mantle composition and processes. Geol Soc London Spec Publ 42: 313–345

Suyehiro K, Takahashi N, Ariie Y, Yokoi Y, Shinohara M, Kanazawa T, Hirata N, Tokuyama H, Taira A (1996) Continental crust, crustal underplating, and low-Q upper mantle beneath an oceanic island arc. Science 272: 390–393

Tatsumi Y, Hamilton DL, Nesbitt RW (1986) Chemical characteristics of fluid phase released from a subducted lithosphere and origin of arc magmas: evidence from high-pressure experiments and natural rocks. J Volcanol Geothermal Res 29: 293–309

Taylor SR, McLennan SM (1985) The continental crust: its composition and evolution. Blackwell Scientific Publications, Oxford

Taylor SR, McLennan SM (1995) The geochemical evolution of the continental crust. Rev Geophys 33: 241–265

Vaughan APM, Millar IL (1996) Early Cretaceous magmatism during extensional deformation within the Antarctic Peninsula magmatic arc. J S Am Earth Sci 9: 121–129

Vaughan APM, Thistlewood L, Millar IL (1995) Small-scale convection at the interface between stratified layers of mafic and silicic magma, Campbell Ridges, NW Palmer Land, Antarctic Peninsula: syn-magmatic way-up criteria. J Struct Geol 17: 1071–1075

Weaver SD, Bruce R, Nelson EP, Brueckner HK, LeHuray AP (1990) The Patagonian batholith at 48°S latitude, Chile; geochemical and isotopic variations. Geol Soc Am Spec Publ 241: 33–50

Wever HE, Millar IL, Pankhurst RJ (1994) Geochronology and radiogenic isotope geology of Mesozoic rocks from eastern Palmer Land, Antarctic Peninsula: crustal anatexis in arc-related granitoid genesis. J S Am Earth Sci 7: 69–83

Wever HE, Storey BC, Leat PT (1995) Peraluminous granites in NE Palmer Land, Antarctic Peninsula: early Mesozoic crustal melting in a magmatic arc. J Geol Soc London 152: 85–96

Willan RCR, Swainbank IG (1995) Galena lead isotopic variations in a Mesozoic–Cenozoic Andean arc, Antarctic Peninsula. J Geol Soc London 152: 767–778

Winther KT (1996) An experimentally based model for the origin of tonalitic and trondhjemitic melts. Chem Geol 127: 43–59

Wolf MB, Wyllie PJ (1993) Garnet growth during amphibolite anatexis: implications of a garnetiferous restite. J Geol 101: 357–373

Wolf MB, Wyllie PJ (1994) Dehydration melting of amphibolite at 10 kbar: the effects of temperature and time. Contrib Mineral Petrol 115: 369–383